^{1}H-CEST and ^{19}F MRI of temperature-responsive liposomal contrast agents for image guided drug delivery

J. Keupp[1], S. Langereis[2], I. de Roos[2], D. Burdinski[2], J. Pikkemaat[2], and H. Gruell[2,3]

[1]Philips Research Europe, Hamburg, Germany, [2]Philips Research Europe, Eindhoven, Netherlands, [3]Eindhoven University of Technology, Eindhoven, Netherlands

Introduction

Localized delivery of anti-cancer drugs based on liposomal nanocarriers [1] promises a larger therapeutic window with reduced side effects of the treatment. If the drug is released from the liposomal nanocarrier locally by external stimulation, *e.g.* temperature or pH [2], therapy is expected to be particularly effective. Temperature-sensitive liposomes release an encapsulated payload near the melting temperature (T_m) of their lipid membrane, e.g. in response to a mild hyperthermic treatment (39-42°C). The present imaging study is based on a new type of temperature-responsive liposomes [3], which are dually labeled for ^{1}H lipoCEST and ^{19}F MR imaging. In their lumen, these liposomes contain both, a chemical shift agent (for ^{1}H lipoCEST detection) as well as a fluorine compound (NH_4PF_6 for ^{19}F detection). Inside the liposome, the ^{19}F spectral lines are strongly broadened and not detectable. This is due to fast relaxation in the non-spherical lumen induced by the paramagnetic chemical shift agent. Upon reaching T_m, the lipoCEST contrast vanishes, due to the release of the chemical shift agent. Simultaneously, the ^{19}F MR signal is visible only after release from the nanocarrier, as it is no longer influenced by the paramagnetic shift agent. Hence, the ^{19}F signal could be used to quantify the amount of released drug payload, while the CEST signal could measure the local nanocarrier concentration before the release. The study demonstrates the potential of dually labeled temperature-sensitive liposomal nanocarriers for MRI-guided drug delivery in cancer therapy.

Methods

The temperature-sensitive liposomes (MPPC/DPPC/DPPE-PEG2000 : 10/90/4) contained 65 mM of [Tm(hpdo3a)(H_2O)] as a chemical shift agent [4], and NH_4PF_6 (50 mM). These liposomes were prepared using lipid film hydration, sequential extrusions through polycarbonate filters and dialysis, which resulted in osmotically shrunken, non-spherical liposomes [5]. For the MR imaging set-up, a 5 mL tube was immersed into a water beaker resting on a resistive heater. Temperature was changed by adding small amounts of hot water, sustained by the heater and monitored to a precision of 0.1°C with a fluoro-optic thermometer (Luxtron 790, LumaSense Technologies, CA). The study was performed on a 3T clinical whole-body scanner (Achieva, Philips Medical Systems) using a dual-tuned transmit/receive RF coil (∅ 7cm) and a dual ^{19}F/^{1}H spectrometer system [6]. With a saturation power of 3.6 µT at Δω=±1600 Hz (varying offset used for z-spectra), 2D lipoCEST images were recorded with a single-shot fast spin echo sequence within 75 s (24 averages, resolution 0.8 mm, matrix 128^2, FOV 100 mm, TR/TE=1571/5.4 ms, pixel bandwidth 374 Hz). A 2D gradient-echo technique was used to image NH_4PF_6 within 200 s (512 averages, 1.9 mm resolution, FOV 120 mm, TR=6.1/3.05 ms, pixel bandwidth 250 Hz).

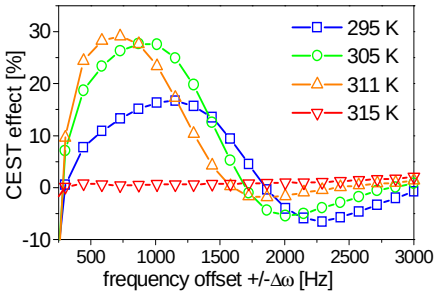

Figure 1: Assessment of temperature-depended lipoCEST effect derived from image based Z-spectra. With increasing temperature, the optimal CEST parameters vary significantly. At the melting phase transition of the liposomes above 311 K, the CEST effect vanishes abruptly.

Results and Discussion

Figure 1 shows the lipoCEST effect (CEST% = ($I_{+\Delta\omega}$ - $I_{-\Delta\omega}$) / $I_{-\Delta\omega}$) versus frequency offset of the saturation pulses and for various temperatures during the heating process (single cycle, not reversible) derived by ROI analysis form a Z-spectral series of 2D CEST images. The maximum CEST effect increases from 17% at 295K (Δω=±1154 Hz) to 29% at 311K (Δω=±728 Hz). At slightly higher temperature, it quickly drops to 0%, indicating the release of the chemical shift agent from the aqueous lumen of the liposome. This Z-spectral analysis was used to adjust the frequency set-point for CEST imaging, which was chosen to Δω=±728 Hz for optimal sensitivity. Here, the CEST signal increases up to T_m , so it will be optimal at physiological temperatures, and steeply drops with mild hyperthermia. Figure 2, shows the CEST images in the upper row, using a color scale for the quantitative CEST percentage. Following average values were observed in an ROI within the tube: 13.3±0.6 % (295K), 26.4±1.0 % (305K), 29.2±1.2 % (311K) and 0.4±0.9 % (315K). At temperatures of 311 K and below, no ^{19}F signal is observed in the images (Figure 2, lower row) as well as in single-voxel spectra (data not shown). At 315 K, the released NH_4PF_6 is clearly visible in images and spectra. Two spectral lines were observed at offset frequencies of 12820 and 12160 Hz. The echo time of 3.05 ms was chosen to acquire the ^{19}F MR signal components in phase, with a chemical shift of 2.6 pixels (components overlap at the bright center).

Conclusion

Feasibility of MR imaging of a ^{1}H-CEST/^{19}F dual-labeled temperature-responsive liposomal nanocarrier was demonstrated in phantom experiments. While the CEST label shows high detectability, the performance of the internalized ^{19}F label has to be optimized for sufficient sensitivity for *in vivo* applications. Time efficient image acquisition could be performed using simultaneous ^{19}F and ^{1}H-CEST imaging [7].

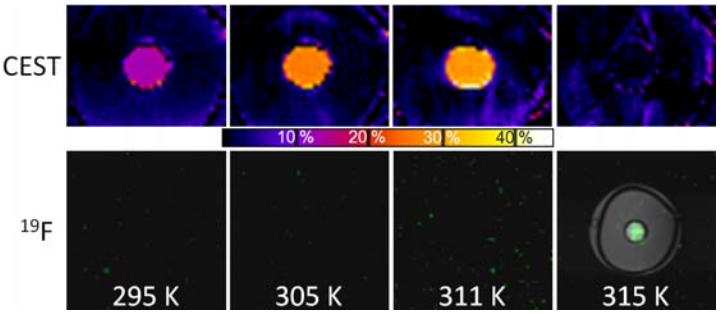

Figure 2: ^{1}H lipoCEST and ^{19}F MR images of temperature-responsive liposomes on a clinical 3.0 T scanner (Achieva, Philips Healthcare). The CEST signal (color scale in percent) vanishes at T ≥311 K, while the fluorine signal appears at 315 K (in green, overlay with ^{1}H image for co-localization and clarity).

References

1. Torchilin, V. P. Nat. Rev. Drug Discovery 4: 145 (2005).
2. Yatvin, M. B et al., M. Science 210: 1253 (1980).
3. Langereis S. et al, submitted to JACS
4. Aime, S. et al., J. Am. Chem. Soc. 129: 2430 (2007).
5. Terreno E. et al., Angew. Chem. Int. Ed. 45: 1 (2006).
6. Keupp J et al., Proc. ISMRM 14: 102 (2006).
7. Keupp J et al., Proc. ISMRM 16: 637 (2008).